Ethylene carbonylation to 3-Pentanone with in-situ hydrogen via water-gas-shift reaction on Rh/CeO_2

Kun Zhang[1,2], Qiang Guo*[2], Yehong Wang[2], Pengfei Cao[3,4], Jian Zhang[2], Marc Heggen[3], Joachim Mayer[3,4], Rafal E. Dunin-Borkowski[3] and Feng Wang*[1,2]

1. Henan Institute of Advanced Technology, College of Chemistry, Zhengzhou University, 450001 Zhengzhou, China.
2. State Key Laboratory of Catalysis, Dalian National Laboratory for Clean Energy, Dalian Institute of Chemical Physics, Chinese Academy of Sciences, 457 Zhongshan Road, 116023 Dalian, China.
3. Ernst Ruska Centre for Microscopy and Spectroscopy with Electrons and Peter Grünberg Institute, Forschungszentrum Juelich GmbH, Juelich 52425, Germany
4. Central Facility for Electron Microscopy, RWTH Aachen University, Aachen 52074, Germany

To whom correspondence should be addressed. E-mail: qguo@dicp.ac.cn; wangfeng@dicp.ac.cn

Abstract

Alkene carbonylation, in which hydrogenation plays pivotal roles, is one of the most efficient ways for the production of oxygenated chemicals like aldehyde, amide and ester etc. In this work, by using in-situ produced hydrogen via water-gas-shift (WGS) reaction, selective ethylene carbonylation to 3-pentanone was achieved instead of hydroformylation to propionaldehyde with gaseous H_2 on a defective ceria supported Rh catalyst. The interface of Rh/CeO_2 which consists of oxygen vacancy and positively charged Rh activates water, CO and ethylene and the subsequent reactions including WGS reaction and ethylene carbonylation. The lean hydrogen circumstance created by WGS reaction which suppresses the hydrogenation of the propionyl group and promotes its ethylation to 3-pentanone. Redox pathway was proposed for WGS reaction based on the in-situ FTIR results and the origin of hydrogen for ethylene carbonylation is water as confirmed by mass spectrometry (MS) study by using d_2-water as one of the reactants. This work provides a promising way for heavier ketone synthesis.

Introduction

Alkene carbonylation is one of the most important ways for the production of value-added chemicals [1-5] and two key steps are involved: CO insertion and sequential reaction of the acyl group.[4] The former step allows addition of one carbonyl group to the carbon chain and the latter one determines the nature of the products. For example, alcoholysis of the acyl group produces ester, [5-6] while hydrogenation of the acyl group produces aldehyde which is known as hydroformylation.[1] Insertion of CO followed by creation of C-C bond holds the promise to produce ketone,[7-8] which is another important family of organic compounds and widely used as solvents, polymer precursors, and pharmaceuticals.[9] For instance, 3-pentanone is always used as a solvent in paint and a precursor to vitamin E and current production of 3-pentanone from ethylene follows a two-step process involving ethylene hydroformylation to propanal, followed by propanal ketonization to 3-pentanone under oxidative conditions.[10-11] Ethylene hydroformylation always generates 3-pentanone as one of the byproducts which provides a potential route for one-step synthesis of 3-pentanone if the main product of ethylene hydroformylation can be tuned toward 3-pentanone instead of propanal (Scheme S1).[12-13] Recently, Sun et al. reported that, on a single-atom Ru catalyst, the selectivity of 3-pentanone in ethylene hydroformylation can be greatly improved due to the lower energy barrier of propionyl ethylation compared with that of

propionyl hydrogenation.[14] However, propionyl hydrogenation overwhelming dominates which always produces propanal as the main product due to the surplus hydrogen on Rh catalysts at ethylene hydroformylation conditions (Scheme 1, route 1-1 to 3-1). For example, Takahashi and coworkers discovered that Rh/Active carbon was an effective catalyst for 3-pentanone production via ethylene hydroformylation but still as the minor product.[15]

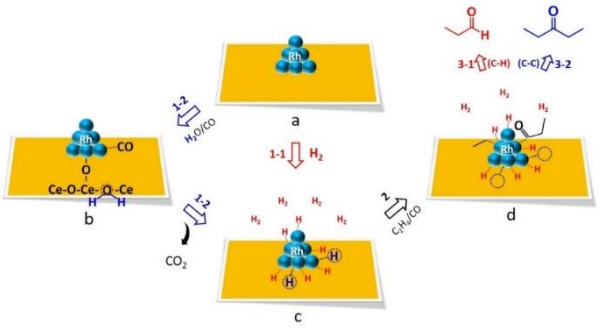

Scheme 1. Ethylene carbonylation with H_2 (red) or in-situ produced H (blue) via water-gas-shift (WGS) reaction.

In-situ generated hydrogen, which is widely used for selective hydrogenation reactions,[16-17] holds the promise to suppress the propionyl hydrogenation and boost the ethylation of propionyl group to 3-pentanone. Coupled with alcohol dehydrogenation-transfer-hydrogenation, ethylene carbonylation to 3-pentanone was attained with production of 1,1-diethoxyethane or acetone[8] as the byproduct and water-gas-shift (WGS) reaction in which water acts as a clean hydrogen source, is one of the most important processes for on-site hydrogen production. Ceria supported metal catalysts show excellent performance for WGS reaction due to their unique properties like the interfacial sites

constructed by ceria oxygen vacancy and the positively charged metal.[18-21] Two different mechanisms, redox and formate processes, were proposed for the low temperature WGS reaction on ceria supported metal catalysts.[18, 20, 22-24] For example, Gorte et al. proposed that metal activated CO was oxidized by lattice oxygen of ceria and the reduced ceria with oxygen vacancies, in turn, was oxidized by H_2O,[20] while Rodriguez et al. reported that formate which decomposed to CO_2 and H_2 was the key intermediate.[25-26] But both mechanisms agree that CO and H_2O were, respectively, activated on the supported metal and oxygen vacancies of ceria (Scheme 1b) and it is well-known that alkene is activated on the supported metal which highlight the crucial roles of the interface of ceria supported metal catalysts.

In this work, by using the in-situ generated hydrogen via WGS reaction, selective ethylene carbonylation to 3-pentanone was achieved on a defective Rh/ceria (Scheme 1, route 1-2 to 3-2). CO and water were activated on positively charged Rh and oxygen vacancies, respectively, and the WGS reaction proceeds via a redox pathway as the hydrogencarbonate species were merely observed in the in-situ FTIR spectra. Mass spectrometry study with d_2-water confirmed that the hydrogen source for ethylene carbonylation to 3-pentanone truly originated from water and this route provides an alternative method for producing heavier ketone via alkene carbonylation.

Results and discussion

In-situ FTIR spectroscopy was firstly used to study the WGS reaction on Rh/CeO_2 at near carbonylation reaction conditions and the in-situ FTIR spectra collected are shown in Figure 1. Besides the bands at 2085 and 2015 cm^{-1} which are attributed to the positively charged Rh carbonyl species and the band at 2070 cm^{-1} which is ascribed to the linear-CO adsorbed on Rh^0 (Figure 1a),[27] two bands at 2360 and 2340 cm^{-1} which arise from CO_2 were also observed once the reaction was started at 160 ^oC (Figure 1b). Moreover, a broad band centered at 1616 cm^{-1} which is assigned to the hydrogencarbonate species appeared and other bands ranging from 1300 to 1500 cm^{-1} are attributed to the carbonate species.[28] With prolonging the reaction time, the band at 1616 cm^{-1} firstly became stronger and then gradually weakened which indicates that the hydrogencarbonate species is a vital intermediate (Scheme S2). Meanwhile, intensity of the bands at 2085 and 2015 cm^{-1} which are from the positively charged Rh carbonyl species decreased, while the band at 2070 cm^{-1} which arises from the Rh^0 carbonyl species kept almost unchanged. In addition, the CO_2 related bands at 2360 and 2340 cm^{-1} gets stronger, while no band related to the formate was observed. The bands at 2085 and 2015 cm^{-1} disappeared after 20 mins of reaction and, concurrently, the band at 1616 cm^{-1} started to weaken. This implies that the hydrogencarbonate species was produced from CO adsorbed on the

positively charged Rh. A new band at 1533 cm^{-1} which is ascribed to the unidentate carbonates was observed and this band along with the carbonates bands at 1330, 1444 and 1480 cm^{-1} became stronger with extending the reaction time. After evacuation, the gaseous CO_2 was removed while the adsorbed species on the catalyst like the carbonates and Rh^0 carbonyl species remain almost intact. These results demonstrate that WGS reaction proceeds via a redox pathway in which hydrogencarbonate species is generated as a key intermediate and the interfacial positively charged Rh activates CO for WGS reaction on Rh/CeO_2 at near carbonylation conditions.

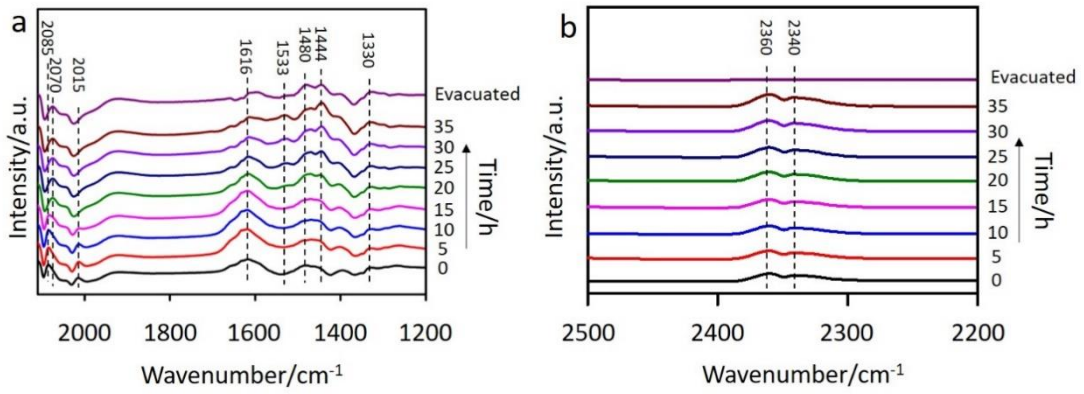

Figure 1. In-situ FTIR spectra of WGS reaction on Rh/CeO_2.

Rh/CeO_2 was then used for ethylene carbonylation with H_2 or in-situ produced hydrogen via WGS reaction. Propionaldehyde was produced as the major product which process is well known for hydroformylation when gaseous H_2 (0.5 MPa) was used as the hydrogen source (Figure 2a). The selectivity of 3-pentanone increased with lowering the H_2 pressure and 60 $mmol/mmol_{Rh}$ 3-pentanone was obtained at t=4 h with a selectivity of 65 %

when 0.1 MPa H_2 was used. When H_2O was used as the sole hydrogen source via WGS reaction, as expected, high selectivity (92 %) of 3-pentanone was achieved although the lean hydrogen circumstance results in the lowered yield of 3-pentanone (36 mmol/$mmol_{Rh}$) at t=4 h. With prolonging the reaction time, the yield of 3-pentanone increased with almost unchanged selectivity and 3-pentanone yield can reach 80 mmol/$mmol_{Rh}$ with 13 mmol/$mmol_{Rh}$ propionaldehyde at t=24 h (Figure 2b). No carbonylation products were observed over bare CeO_2 (not shown for clarity) and only trace amounts of carbonylation products were produced on SiO_2 and TiO_2 supported Rh catalysts and ceria supported Ru and Pt catalysts (Figure S1).

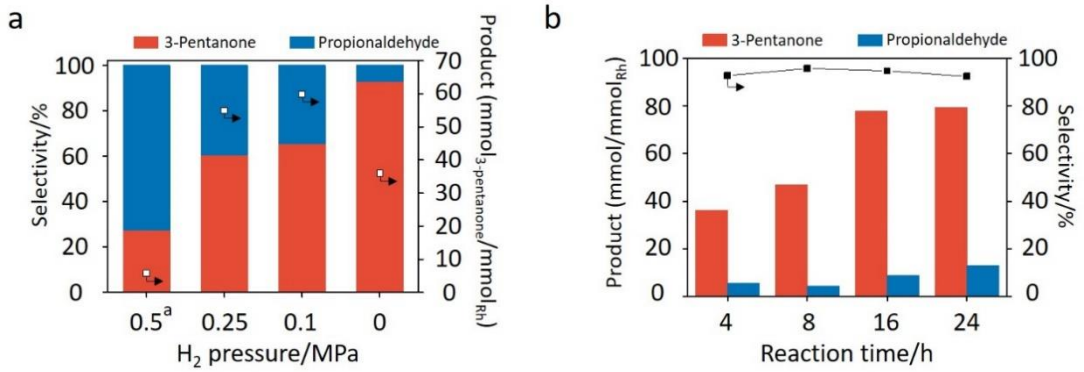

Figure 2. Ethylene carbonylation on Rh/CeO_2 at different H_2 pressure (a); various reaction times (b). (Reaction conditions: 50 mg Rh/CeO_2, 3 mmol ethylene, 1.5 MPa H_2/CO, 3 ml 1,4-dioxane, 0.15 ml water, 1 mmol n-Dodecane as the internal standard, 160 °C, 4 h; a: no water was added)

To confirm the participation of water and CO, various amounts of water and CO pressures were used to study their effects on both the yield and selectivity of 3-pentanone (Figure 3a and b). Limited amount of 3-pentanone (18 mmol/$mmol_{Rh}$) was obtained when 2 % water was used, although the selectivity was high (95 %). With increasing the water

amount, the selectivity kept unchanged and yield gradually increased. Up to 80 $mmol_{3\text{-pentanone}}/mmol_{Rh}$ was produced when 20 % water was added. In regular water, the molecular ion peak of 3-pentanone was m/z=86 and the strongest ion peak was m/z=57 which belongs to the fragment ion of CH_3CH_2CO-(Figure 3d). When the water was replaced by D_2O, the molecular ion peak of 3-pentanone moved to m/z=88 and the m/z=58 was the strongest ion peak which could be assigned to the fragment ion of $C(D)H_2CH_2CO$-(Figure 3e). The isotopic tracing experiments confirmed that the H for ethylene carbonylation originated from water and located at the C(1) and C(5) sites of 3-pentanone and C(1) and C(3) sites of propionaldehyde which was produced by ethylene hydroformylation as the byproduct (Figure S2). Increasing the CO pressure also boosted the production of 3-pentanone and the yield of 3-pentanone was increased from 15 to 55 $mmol/mmol_{Rh}$ when 1.5 MPa CO was charged into the reactor instead of 0.5 MPa (Figure 3b). The effect of temperature was also studied and it was found that the highest yield of 3-pentanone (36 $mmol/mmol_{Rh}$) was obtained when the reaction was done at 160 ^{o}C (Figure 3c). This should come from the fact that elimination reaction on Rh, which is an exothermic reaction, is unfavorable at higher temperature.

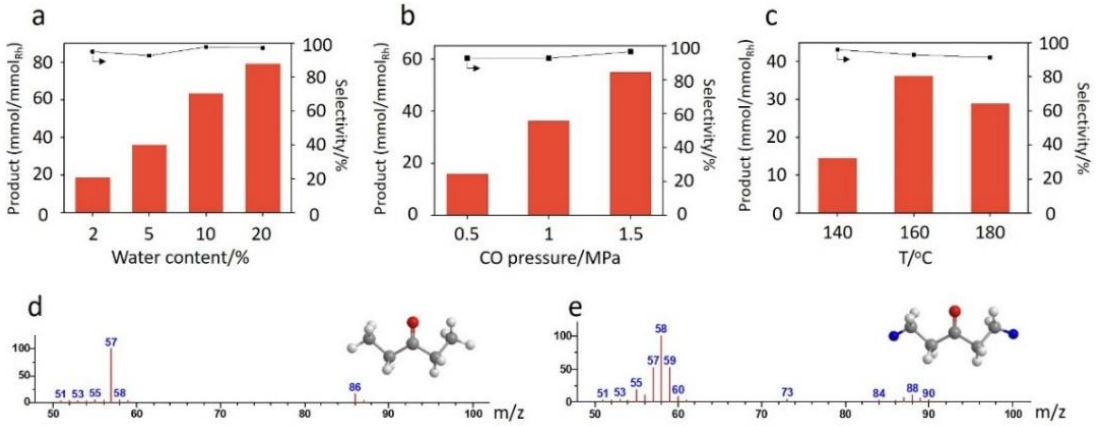

Figure 3. Ethylene carbonylation on Rh/CeO_2 at various reaction conditions: different water contents (a); different CO pressure (b) and different temperature (c). Mass spectra of 3-pentanone produced from ethylene carbonylation with H_2O (d) and D_2O (e). (Reaction conditions: 50 mg Rh/CeO_2, 3 mmol ethylene, 1.5 MPa CO, 3 ml 1,4-dioxane, 0.15 ml water except a, 1 mmol n-Dodecane as the internal standard, 160 °C, 4 h)

Figure 4a-d show scanning transmission electron microscopy (STEM) images of the Rh/CeO_2 and corresponding spatially resolved energy dispersive X-ray (EDX) maps of the Rh/CeO_2 are exhibited in Figure 4e-h. Dark field (DF) and secondary electron (SE) STEM images show that ceria particle size is around 10 nm and a few small Rh nanoparticles (about 2 nm in diameter, in Figure S3) are located on the surface of ceria. Highly dispersed Rh species with trace amounts of small Rh nanoparticles were also revealed by EDX-mapping of the Rh/CeO_2 and this is in accordance with the FTIR study which indicates that both positively charged and metallic Rh are present on ceria.

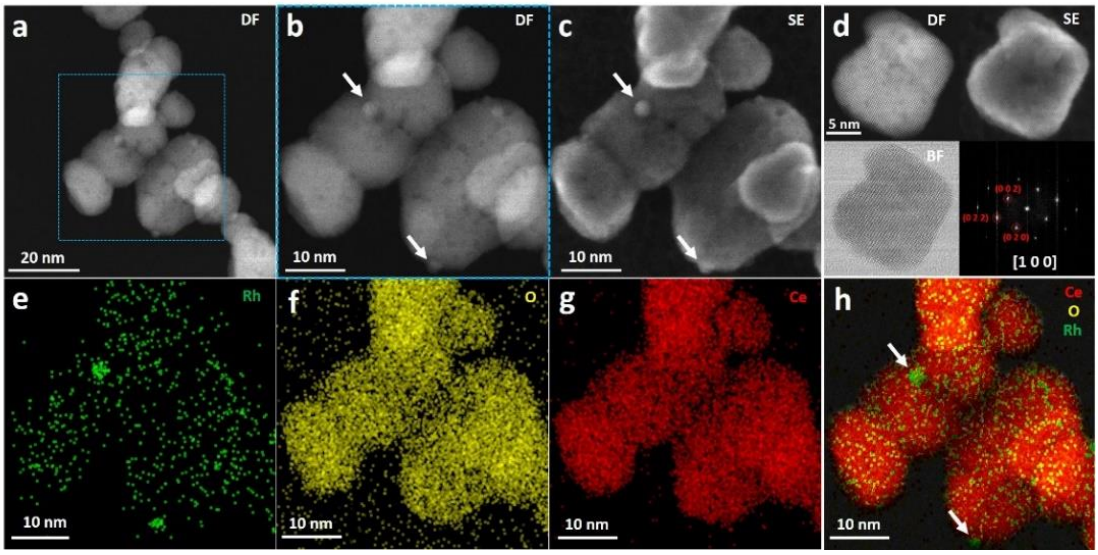

Figure 4. Dark field (DF), bright field (BF), and secondary electron (SE) STEM images (a-d) and corresponding EDX elemental mapping of Rh (e), O (f), Ce (g) and Rh + O +Ce mixture of Rh/CeO_2 catalyst

Raman spectra of Rh/CeO_2 and bare CeO_2 are shown in Figure 5a. Two characteristic Raman bands at 592 cm^{-1} and 462 cm^{-1}, which are assigned to the defect-induced mode and F2g mode of CeO_2 respectively,[29-30] were observed. The relative intensity ratio of I_{592}/I_{462} was significantly enhanced after Rh was supported on ceria. This comes from the fact that metal-support interactions between Rh and ceria greatly promotes the interfacial oxygen vacancy formation via $Rh^{\delta+}$-O-Ce-O_v-Ce.[8, 31-32] When ethylene was adsorbed on the Rh/CeO_2, three IR bands at 2875 cm^{-1}, 2940 cm^{-1} and 2960 cm^{-1} which were assigned to the di-σ-bonded ethylene appeared and this indicates that ethylene mainly adsorbed on the highly dispersed Rh clusters or nanoparticles (Figure S4). Figure 5b and 5c show the IR spectra of adsorbed pyridine on Rh/CeO_2 before and after water adsorption, respectively. In addition to the bands attributed to Lewis acid sites (1444, 1486 and 1595 cm^{-1}), only a faint peak at 1537 cm^{-}

[1] which was assigned to the pyridine adsorbed on Brønsted acid sites and a weak shoulder peak at 1580 cm^{-1} corresponding to H-bonded pyridine were observed on Rh/CeO_2 without water pre-adsorption.[33-34] After water was pre-adsorbed on the Rh/CeO_2 catalyst, the peak at 1537 cm^{-1} and 1580 cm^{-1} became stronger. But no pyridine adsorbed on Brønsted acid sites was observed when water was pre-adsorbed on pure CeO_2 (Figure S5). This indicates that interfacial oxygen vacancies of Rh/CeO_2 promotes the dissociatively adsorption of water.

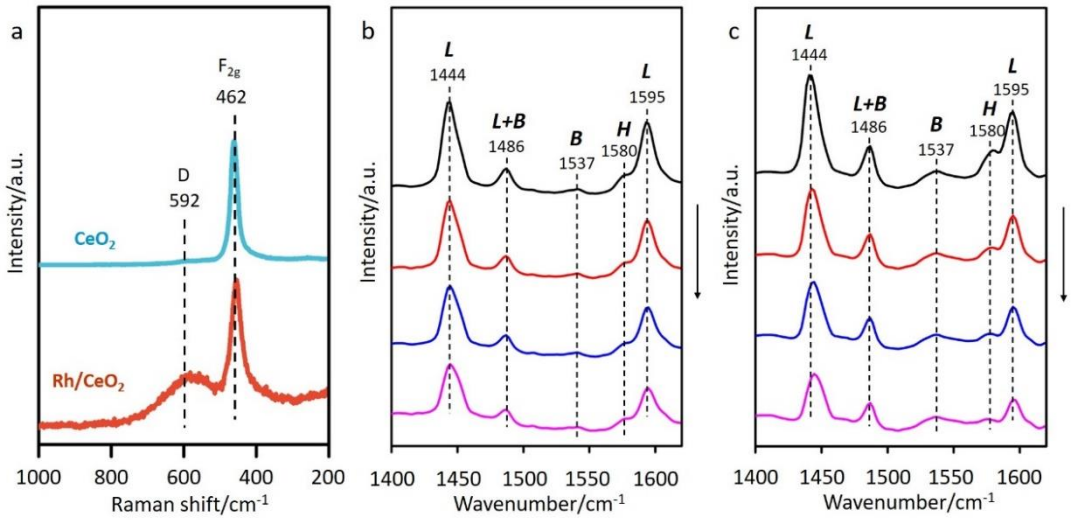

Figure 5. Raman spectra of Rh/CeO_2 and CeO_2 excited at 532 nm (a), FTIR spectra after pyridine adsorption and evacuation in vacuo on Rh/CeO_2 before (b) and after (c) water adsorption (The arrow indicates desorbing sequence of pyridine in vacuo).

Based on our results, we proposed the following pathway for ethylene carbonylation to 3-pentanone with in-situ produced H via WGS reaction on defective Rh/CeO_2 (Scheme 2): firstly, water was dissociatively adsorbed on the oxygen vacancy of ceria, while CO and ethylene were activated on Rh. The CO on positively charged Rh reacted with the hydroxyl groups produced from water to generate hydrogencarbonate

species. Then the hydrogencarbonate species decomposed: H was transferred onto the Rh surface and oxygen vacancy of ceria restored when CO_2 was released from the ceria surface. The activated ethylene captured the H on Rh from water to form ethyl group followed by CO insertion. The generated propionyl group finally reacted with another ethyl group to produce 3-pentanone and if surplus H covered the Rh surface, like H_2 was used as the H source, the propionyl group would be hydrogenated to propionaldehyde.

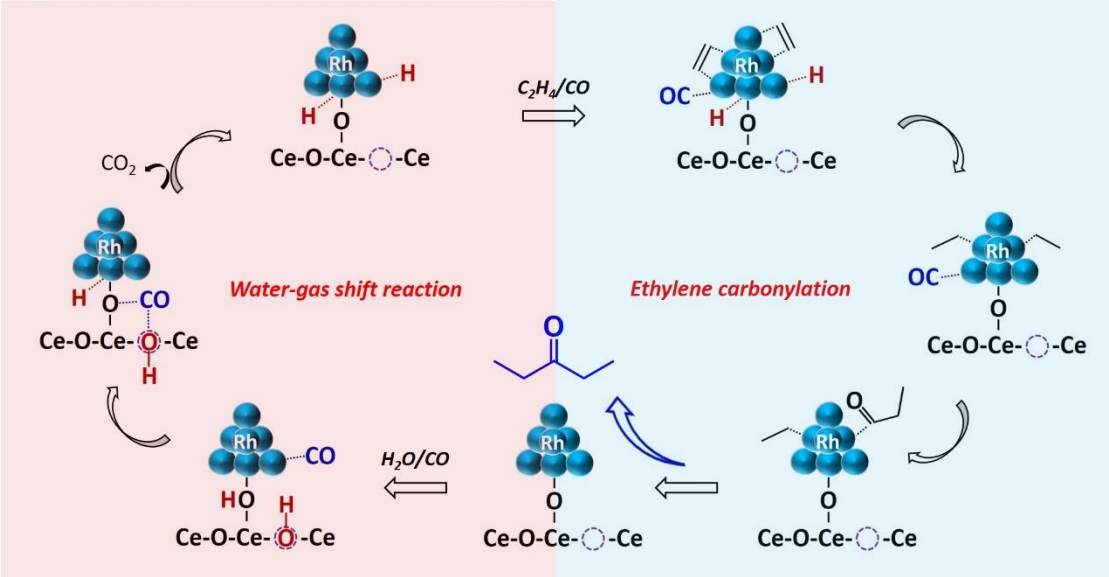

Scheme 2. Proposed mechanism of ethylene carbonylation coupled with water-gas shift reaction to 3-pentanone on defective Rh/CeO_2.

Conclusion

Coupled with water-gas-shift (WGS) reaction, highly selective ethylene carbonylation to 3-pentanone was achieved on a defective ceria supported Rh catalyst. Water, which donates the hydrogen for ethylene carbonylation as confirmed by MS study, is dissociated on the oxygen

vacancies of ceria, CO is activated on positively charged Rh and the subsequent steps for WGS reaction proceed via a redox mechanism as revealed by the in-situ FTIR study. When gaseous H_2 was involved, the selectivity of 3-pentanone decreased due to the parallel reaction of ethylene hydroformylation which underlines the key role of lean hydrogen produced via WGS reaction for selective hydrogenation. This work opens an alternative route for heavier ketone synthesis.

References:

1. Franke, R.; Selent, D.; Borner, A., Applied Hydroformylation. *Chem. Rev.* **2012,** *112* (11), 5675-5732.
2. Kiss, G., Palladium-catalyzed Reppe carbonylation. *Chem. Rev.* **2001,** *101* (11), 3435-3456.
3. Wu, X. F.; Neumann, H.; Beller, M., Synthesis of Heterocycles via Palladium-Catalyzed Carbonylations. *Chem. Rev.* **2013,** *113* (1), 1-35.
4. Peng, J. B.; Geng, H. Q.; Wu, X. F., The Chemistry of CO: Carbonylation. *Chem-Us* **2019,** *5* (3), 526-552.
5. Yang, J.; Liu, J. W.; Neumann, H.; Franke, R.; Jackstell, R.; Beller, M., Direct synthesis of adipic acid esters via palladium-catalyzed carbonylation of 1,3-dienes. *Science* **2019,** *366* (6472), 1514-1517.
6. An, J. H.; Wang, Y. H.; Lu, J. M.; Zhang, J.; Zhang, Z. X.; Xu, S. T.; Liu, X. Y.; Zhang, T.; Gocyla, M.; Heggen, M.; Dunin-Borkowsk, R. E.; Fornasiero, P.; Wang, F., Acid-Promoter-Free Ethylene Methoxycarbonylation over Ru-Clusters/Ceria: The Catalysis of Interfacial Lewis Acid-Base Pair. *J. Am. Chem. Soc.* **2018,** *140* (11), 4172-4181.
7. Wu, F. P.; Yuan, Y.; Liu, J. W.; Wu, X. F., Pd/Cu-Catalyzed Defluorinative Carbonylative Coupling of Aryl Iodides and gem-Difluoroalkenes: Efficient Synthesis of alpha-Fluorochalcones. *Angew. Chem. Int. Edit.* **2021,** *60* (16), 8818-8822.
8. Guo, Q.; Wang, Y. H.; Han, J. Y.; Zhang, J.; Wang, F., Interfacial Tandem Catalysis for Ethylene Carbonylation and C-C Coupling to 3-Pentanone on Rh/Ceria. *ACS Catal.* **2022,** *12* (6), 3286-3290.
9. Chalotra, N.; Sultan, S.; Shah, B. A., Recent Advances in Photoredox Methods for Ketone Synthesis. *Asian J Org Chem* **2020,** *9* (6), 863-881.
10. Renz, M., Ketonization of carboxylic acids by decarboxylation: Mechanism and scope. *Eur J Org Chem* **2005,** *2005* (6), 979-988.
11. Kamimura, Y.; Sato, S.; Takahashi, R.; Sodesawa, T.; Fukui, M., Vapor-phase synthesis of symmetric ketone from alcohol over CeO2-Fe2O3 catalysts. *Chem Lett* **2000,** (3), 232-233.
12. Gorbunov, D. N.; Nenasheva, M. V.; Matsukevich, R. P.; Terenina, M. V.; Putilin, F. N.; Kardasheva, Y. S.; Maksimov, A. L.; Karakhanov, E. A., Ethylene Hydroformylation in the Presence of Rhodium Catalysts in Hydrocarbon-Rich Media: The Stage of Combined Conversion of Refinery Gases to Oxygenates. *Petrol Chem+* **2019,** *59* (9), 1009-1016.
13. Song, X. G.; Ding, Y. J.; Chen, W. M.; Dong, W. D.; Pei, Y. P.; Zang, J.; Yan, L.; Lu, Y., Formation of 3-pentanone via ethylene hydroformylation over Co/activated carbon catalyst. *Appl Catal a-Gen* **2013,** *452*, 155-162.
14. Qin, T. T.; Dang, Y. R.; Lin, T. J.; Mei, B. B.; Wu, B.; Li, X.; Li, S. G.; Jiang, Z.; Tang, Z. Y.; Zhong, L. S.; Sun, Y. H., Single-atom Ru catalyst for selective synthesis of 3-pentanone via ethylene hydroformylation. *Green Chem* **2021,** *23* (22), 9038-9047.
15. Takahashi, N.; Takeyama, T.; Yanagibashi, T.; Takada, Y., Comparison of Pentan-3-One Formation with Propionaldehyde Formation during Ethylene Hydroformylation over Rh Active-Carbon Catalyst. *J Catal* **1992,** *136* (2), 531-538.
16. Hao, C. H.; Guo, X. N.; Pan, Y. T.; Chen, S.; Jiao, Z. F.; Yang, H.; Guo, X. Y., Visible-Light-Driven Selective Photocatalytic Hydrogenation of Cinnamaldehyde over Au/SiC Catalysts. *J. Am. Chem. Soc.* **2016,** *138* (30), 9361-9364.
17. He, L.; Yu, F. J.; Lou, X. B.; Cao, Y.; He, H. Y.; Fan, K. N., A novel gold-catalyzed chemoselective reduction of alpha,beta-unsaturated aldehydes using CO and H2O as the hydrogen source. *Chem*

Commun **2010,** *46* (9), 1553-1555.
18. Montini, T.; Melchionna, M.; Monai, M.; Fornasiero, P., Fundamentals and Catalytic Applications of CeO2-Based Materials. *Chem. Rev.* **2016,** *116* (10), 5987-6041.
19. Rodriguez, J. A.; Grinter, D. C.; Liu, Z. Y.; Palomino, R. M.; Senanayake, S. D., Ceria-based model catalysts: fundamental studies on the importance of the metal-ceria interface in CO oxidation, the water-gas shift, CO2 hydrogenation, and methane and alcohol reforming. *Chem. Soc. Rev.* **2017,** *46* (7), 1824-1841.
20. Bunluesin, T.; Gorte, R. J.; Graham, G. W., Studies of the water-gas-shift reaction on ceria-supported Pt, Pd, and Rh: implications for oxygen-storage properties. *Appl Catal B-Environ* **1998,** *15* (1-2), 107-114.
21. Vecchietti, J.; Bonivardi, A.; Xu, W. Q.; Stacchiola, D.; Delgado, J. J.; Calatayud, M.; Collins, S. E., Understanding the Role of Oxygen Vacancies in the Water Gas Shift Reaction on Ceria-Supported Platinum Catalysts. *Acs Catal* **2014,** *4* (6), 2088-2096.
22. Li, Y.; Fu, Q.; Flytzani-Stephanopoulos, M., Low-temperature water-gas shift reaction over Cu- and Ni-loaded cerium oxide catalysts. *Appl Catal B-Environ* **2000,** *27* (3), 179-191.
23. Shido, T.; Iwasawa, Y., Regulation of Reaction Intermediate by Reactant in the Water Gas Shift Reaction on CeO2, in Relation to Reactant-Promoted Mechanism. *J Catal* **1992,** *136* (2), 493-503.
24. Shido, T.; Iwasawa, Y., Reactant-Promoted Reaction-Mechanism for Water Gas Shift Reaction on Rh-Doped CeO2. *J Catal* **1993,** *141* (1), 71-81.
25. Rodriguez, J. A.; Ma, S.; Liu, P.; Hrbek, J.; Evans, J.; Perez, M., Activity of CeOx and TiOx nanoparticles grown on Au(111) in the water-gas shift reaction. *Science* **2007,** *318* (5857), 1757-1760.
26. Rodriguez, J. A.; Liu, P.; Hrbek, J.; Evans, J.; Perez, M., Water gas shift reaction on Cu and Au nanoparticles supported on CeO2(111) and ZnO(000(1)over-bar): Intrinsic activity and importance of support interactions. *Angew Chem Int Edit* **2007,** *46* (8), 1329-1332.
27. Lang, R.; Li, T. B.; Matsumura, D.; Miao, S.; Ren, Y. J.; Cui, Y. T.; Tan, Y.; Qiao, B. T.; Li, L.; Wang, A. Q.; Wang, X. D.; Zhang, T., Hydroformylation of Olefins by a Rhodium Single-Atom Catalyst with Activity Comparable to RhCl(PPh3)(3). *Angew. Chem. Int. Edit.* **2016,** *55* (52), 16054-16058.
28. Wang, X. Q.; Rodriguez, J. A.; Hanson, J. C.; Gamarra, D.; Martinez-Arias, A.; Fernandez-Garcia, M., In situ studies of the active sites for the water gas shift reaction over Cu-CeO2 catalysts: Complex interaction between metallic copper and oxygen vacancies of ceria. *J Phys Chem B* **2006,** *110* (1), 428-434.
29. Taniguchi, T.; Watanabe, T.; Sugiyama, N.; Subramani, A. K.; Wagata, H.; Matsushita, N.; Yoshimura, M., Identifying Defects in Ceria-Based Nanocrystals by UV Resonance Raman Spectroscopy. *J Phys Chem C* **2009,** *113* (46), 19789-19793.
30. Wu, Z. L.; Li, M. J.; Howe, J.; Meyer, H. M.; Overbury, S. H., Probing Defect Sites on CeO2 Nanocrystals with Well-Defined Surface Planes by Raman Spectroscopy and O-2 Adsorption. *Langmuir* **2010,** *26* (21), 16595-16606.
31. Acerbi, N.; Tsang, S. C. E.; Jones, G.; Golunski, S.; Collier, P., Rationalization of Interactions in Precious Metal/Ceria Catalysts Using the d-Band Center Model. *Angew Chem Int Edit* **2013,** *52* (30), 7737-7741.
32. Mao, M. Y.; Ly, H. Q.; Li, Y. Z.; Yang, Y.; Zeng, M.; Li, N.; Zhao, X. J., Metal Support Interaction in Pt Nanoparticles Partially Confined in the Mesopores of Microsized Mesoporous CeO2 for Highly Efficient Purification of Volatile Organic Compounds. *Acs Catal* **2016,** *6* (1), 418-427.
33. Parry, E. P., An Infrared Study of Pyridine Adsorbed on Acidic Solids Characterization of Surface

Acidity. *J Catal* **1963,** *2* (5), 371-379.

34. Wu, Z. L.; Mann, A. K. P.; Li, M. J.; Overbury, S. H., Spectroscopic Investigation of Surface-Dependent Acid Base Property of Ceria Nanoshapes. *J Phys Chem C* **2015,** *119* (13), 7340-7350.

Supporting information

Ethylene carbonylation to 3-Pentanone with in-situ hydrogen via water-gas-shift reaction on Rh/CeO_2

Kun Zhang[1,2], Qiang Guo*[2], Yehong Wang[2], Pengfei Cao[3,4], Jian Zhang[2], Marc Heggen[3], Joachim Mayer[3,4], Rafal E. Dunin-Borkowski[3] and Feng Wang*[1,2]

1. Henan Institute of Advanced Technology, College of Chemistry, Zhengzhou University, 450001 Zhengzhou, China.
2. State Key Laboratory of Catalysis, Dalian National Laboratory for Clean Energy, Dalian Institute of Chemical Physics, Chinese Academy of Sciences, 457 Zhongshan Road, 116023 Dalian, China.
3. Ernst Ruska Centre for Microscopy and Spectroscopy with Electrons and Peter Grünberg Institute, Forschungszentrum Juelich GmbH, Juelich 52425, Germany
4. Central Facility for Electron Microscopy, RWTH Aachen University, Aachen 52074, Germany

To whom correspondence should be addressed. E-mail: qguo@dicp.ac.cn; wangfeng@dicp.ac.cn

Experimental section

1. Catalyst Preparation

CeO_2 nanoparticles were prepared through a conventional precipitation method. Typically, 15 g $Ce(NO_3)_3 \cdot 6H_2O$ was dissolved in 300 mL DI water. Then ammonia solution was added dropwise to the cerium solution to obtain $Ce(OH)_3$, with the pH value of the resulting solution controlled at around 11. After stirring overnight, the precipitate was washed by filtration. The solid was dried at 70 ^oC overnight and then calcined at 500 ^oC for 4 h in muffle furnace. The Rh/CeO_2 was prepared by wet impregnation method using $RhCl_3 \cdot 3H_2O$ as the Rh source: firstly, 2g CeO_2 nanoparticles was added to an aqueous solution containing certain amount of Rhodium(III) chloride trihydrate. After stirring overnight, the suspension was dried at 120 ^oC under stirring. The solid was calcined at 200 ^oC for 4 h under air atmosphere and then reduced at 200 °C for 4 h in a tube-furnace with H_2.

2. Characterization

HRTEM:

Dark field scanning transmission electron microscopy (DF-STEM) images were acquired on a Hitachi HF5000at Ernst Ruska Centre for Microscopy and Spectroscopy with Electrons and Peter Grünberg Institute (Forschungszentrum Juelich GmbH, Juelich, Germany). The electron microscope was operated at 200 kV, which is a cold FEG TEM/STEM with a Cs probe corrector. Compositional maps were obtained by energy-dispersive X-ray spectroscopy (EDX) analysis using double EDX Ultra 100 detector from Oxford Instruments.

Raman spectroscopy:

Raman spectra were measured on a Renishaw Company spectrograph with spectral

resolution of 2 cm^{-1}. The laser line at 532 nm of a solid laser was used as the exciting source and the power of the laser, measured at the samples, was about 0.3 mW.

Py-IR:

Self-supporting wafers (10-20 mg/cm^2) were pressed and sealed in an IR heatable cell. The sample was reduced with H_2 at 200 ^oC for 0.5 h and cooled to 30 ^oC under dynamic vacuum. At this point, a baseline spectrum was recorded. Then pyridine was introduced and spectra were acquired after the cell was evacuated under dynamic vacuum for every 20 min. To study the water adsorption, water was introduced into the IR cell after it was cooled to 30 ^oC before the baseline spectrum was recorded.

In-situ FTIR:

Self-supporting wafers (10-20 mg/cm^2) were pressed and sealed in a heatable IR cell. The sample was reduced with H_2 at 200 ^oC for 0.5 h and cooled to 30 ^oC under dynamic vacuum. At this point, a baseline spectrum was recorded. Subsequent heating to 160 ^oC was performed at 10 ^oC/min, with a subsequent hold time of 10 min prior to acquisition of another base line spectrum. After the cell cooled to 30 ^oC, water was introduced into the cell by flowing CO through a water bubbler. The cell was heated to 160 ^oC to trigger the reaction and a series of representative FTIR spectra was recorded every 5 min.

GCMS:

Gas chromatograph-mass spectrometer (GC-MS) was measured on Agilent 7890-5975C instrument under the EI ionization model.

3. Catalytic Reactions

The catalytic reactions were carried out in a Teflon-lined stainless-steel autoclave. In a typical procedure, 50 mg catalyst, 3 ml 1,4-dioxane, 1 mmol n-Dodecane as the internal standard and 150 ul water were loaded into the reactor. The reactor was sealed and purged with Ar for three times. Then ethylene and CO were charged into the reactor to a certain pressure. The reactor was placed in a temperature-controlled steel stainless band heater. After quenching the reactor in an ice bath, products were

collected and analyzed by gas chromatography (GC) with an HP-5 column.

Produced 3-pentanone is given as $mmol_{3\text{-pentanone}}/mmol_{Rh}$.

Selectivity is reported relative to all the products detected and given as 100 % *($m_{propanal}$ or $2*m_{3\text{-pentanone}}$)/($2*m_{3\text{-pentanone}}$+ $m_{propanal}$).

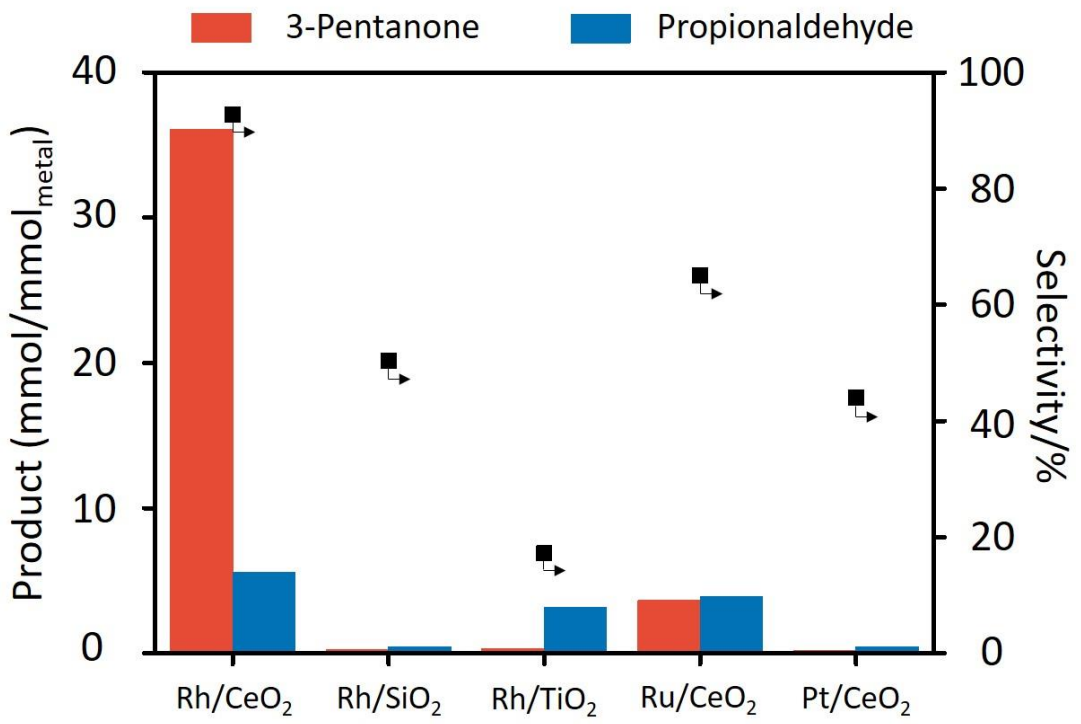

Figure S1. (Reaction conditions: 50 mg catalyst, 3 mmol ethylene, 1.4 MPa CO, 3 ml 1,4-dioxane, 0.15 ml water, 1 mmol n-Dodecane as the internal standard, 160 ^{o}C, 4 h)

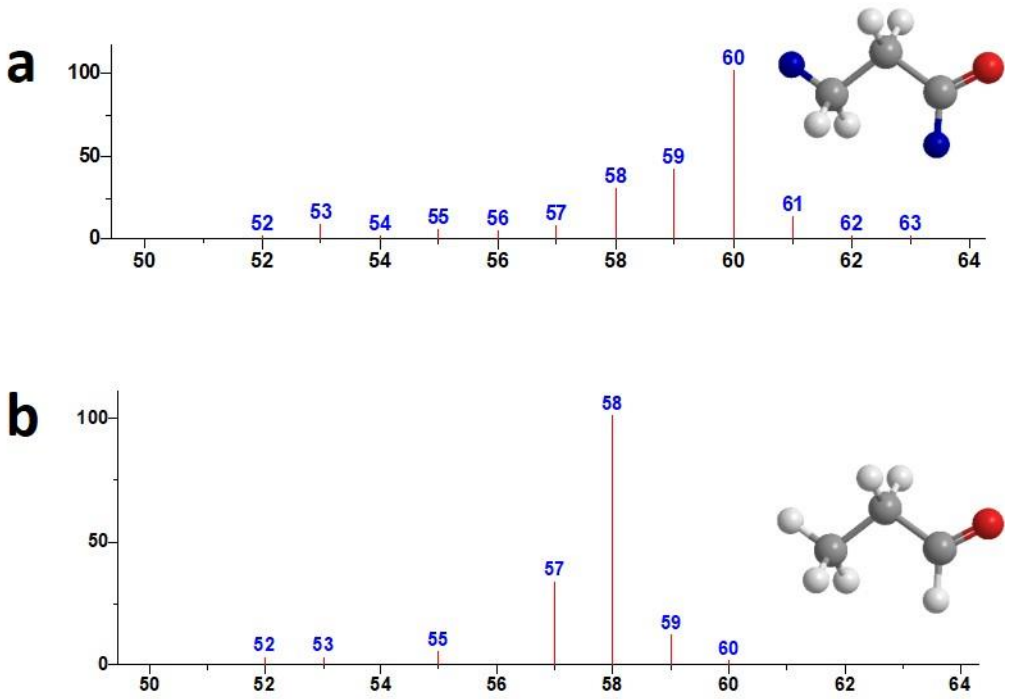

Figure S2. Mass spectra of propylaldehyde produced from ethylene carbonylation with (a) D_2O and (e) H_2O. (Reaction conditions: 50 mg Rh/CeO_2, 3 mmol ethylene, 1.4 MPa CO, 3 ml 1,4-dioxane, 0.15 ml water, 1 mmol n-Dodecane as the internal standard, 160 ^oC, 4 h)

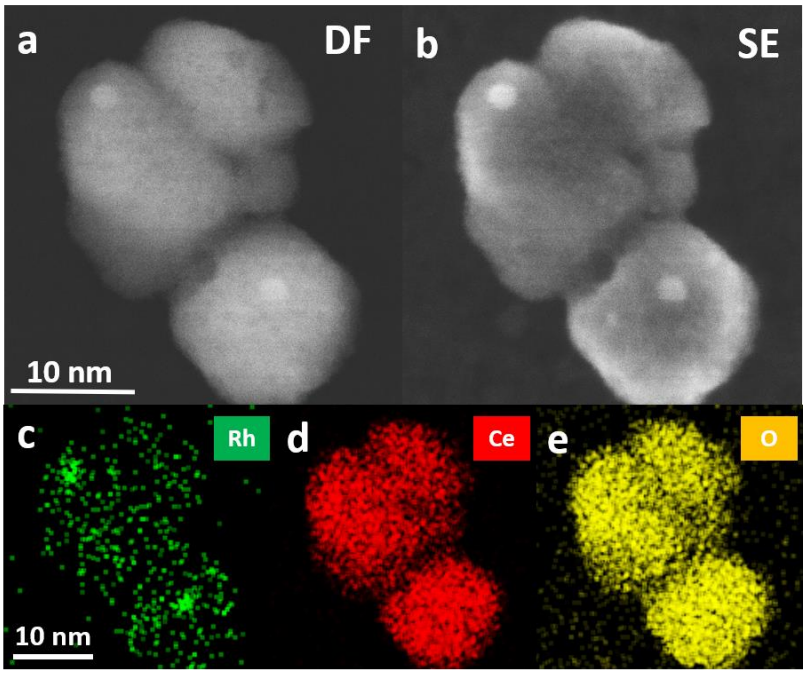

Figure S3. Dark field (DF) and secondary electron (SE) STEM images (a, b) and the corresponding EDX elemental mapping of Rh (c), Ce (d) and O (e) of Rh/CeO2 catalyst

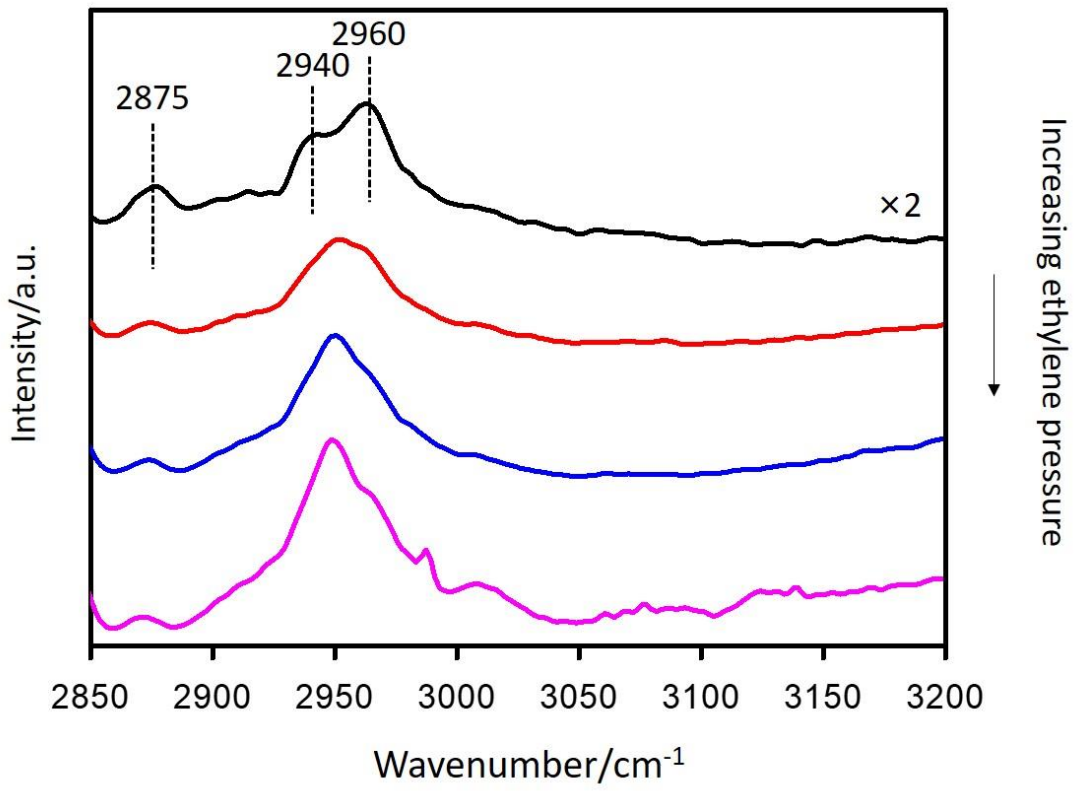

Figure S4. IR spectra of ethylene adsorbed on Rh/CeO_2 in the presence of water.

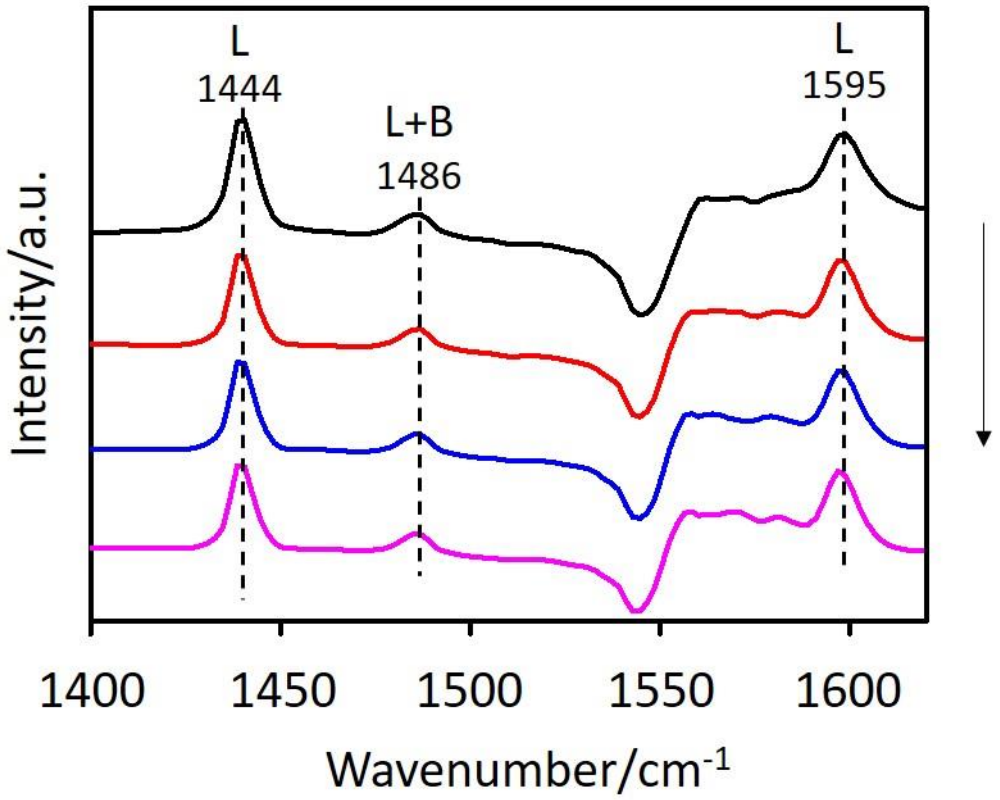

Figure S5. FTIR spectra after pyridine adsorption and evacuation in vacuo on Rh/CeO_2 after water pre-adsorption (The arrow indicates desorbing sequence of pyridine in vacuo).

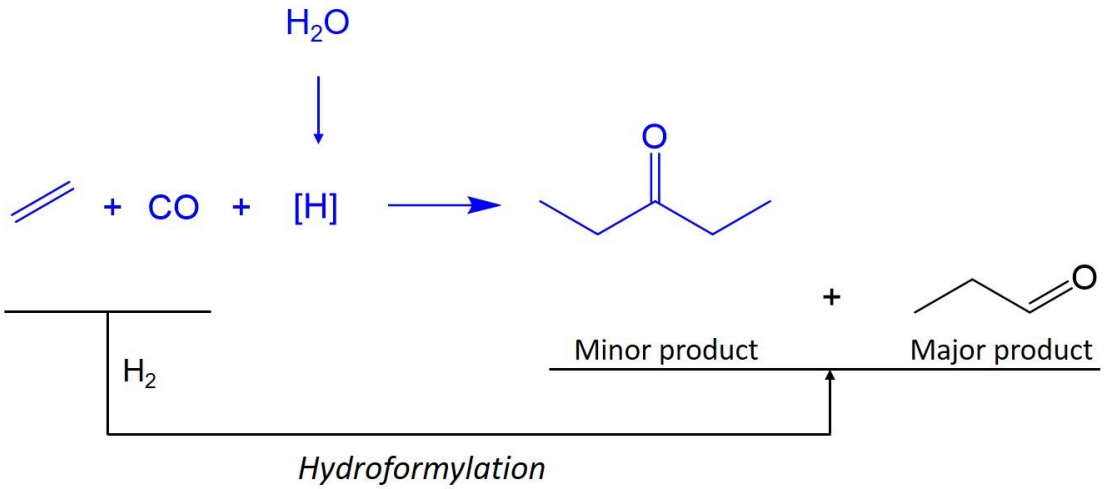

Scheme S1. Schematic ethylene carbonylation to 3-pentanone with in-situ generated H via water gas shift reaction and ethylene hydroformylation with gaseous H_2.

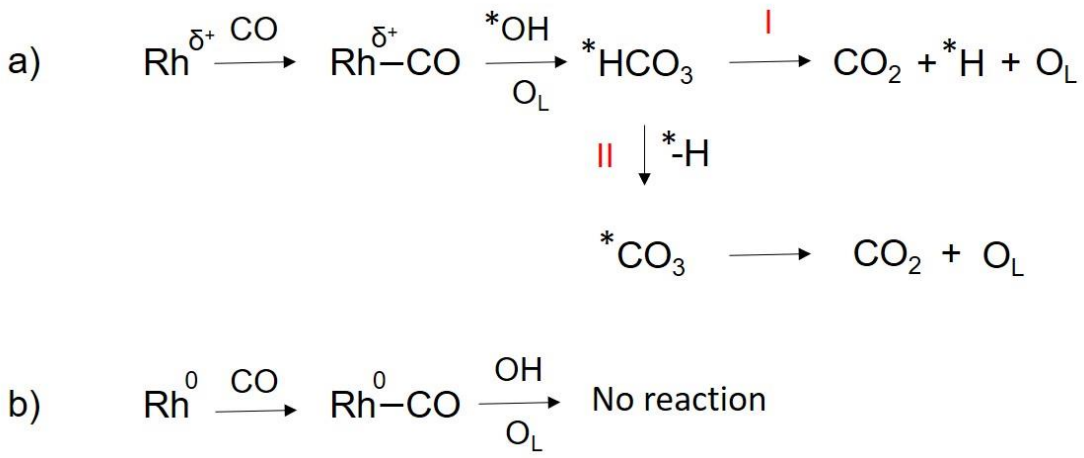

Scheme S2. Proposed water-gas-shift reaction mechanism on Rh/CeO_2.